applied sciences

MDPI

Article

Novel Resveratrol-Inspired Methoxy Carbamates—Synthesis, Selective Butyrylcholinesterase Inhibition and Related Anti-Inflammatory Activity

Milena Mlakić [1,†], Anamarija Raspudić [2,†], Tea Horvat [1], Stanislava Talić [2], Tea Bruketa [3,‡], Danijela Barić [4] and Irena Škorić [1,*]

[1] Department of Organic Chemistry, Faculty of Chemical Engineering and Technology, University of Zagreb, Trg Marka Marulića 19, HR-10 000 Zagreb, Croatia; mdragojev@fkit.unizg.hr (M.M.); thorvat@fkit.hr (T.H.)
[2] Department of Chemistry, Faculty of Science and Education, University of Mostar, Matice Hrvatske bb, 88 000 Mostar, Bosnia and Herzegovina; anamarija.raspudic@fpmoz.sum.ba (A.R.); stanislava.talic@fpmoz.sum.ba (S.T.)
[3] Faculty of Biotechnology and Drug Development, University of Rijeka, Radmile Matejčić 2, HR-51 000 Rijeka, Croatia; tea.bruketa@selvita.com
[4] Group for Computational Life Sciences, Division of Physical Chemistry, Ruđer Bošković Institute, Bijenička Cesta 54, HR-10 000 Zagreb, Croatia; dbaric@irb.hr
* Correspondence: iskoric@fkit.unizg.hr
† These authors contributed equally to this work.
‡ Current address: Pharmacology In Vitro, Selvita Ltd., Prilaz Baruna Filipovića 29, HR-10 000 Zagreb, Croatia.

Abstract

Resveratrol-inspired methoxy-substituted pyrrolidine- and morpholine-based carbamates bearing oxazole or benzimidazole moieties were synthesized and evaluated for their cholinesterase-inhibitory and anti-inflammatory activities. A series of twelve compounds (**1**–**12**) was prepared and structurally characterized using spectroscopic methods. Their inhibitory activities against acetylcholinesterase (AChE) and butyrylcholinesterase (BChE) were determined using a modified Ellman assay, while anti-inflammatory activity was assessed by measuring TNF-α production in lipopolysaccharide-stimulated human peripheral blood mononuclear cells. The investigated compounds selectively inhibited BChE, while showing weak or negligible inhibition of AChE. Pyrrolidine-based oxazole carbamate **1** exhibited the highest BChE inhibitory potency (IC_{50} = 0.09 μM), approximately 25-fold greater than standard rivastigmine. Compound **1** was also the only tested derivative to concentration-dependently inhibit TNF-α production (IC_{50} = 4.3 μM) without affecting cell viability. Molecular docking of compounds **1** and **9**, the best pyrrolidine- and morpholine-based carbamates, indicated that both fit within the BChE active-site gorge through extensive aromatic, hydrophobic, and polar interactions. Overall, the results identify compound **1** as a promising multifunctional lead for further investigation of the relationship between cholinesterase inhibition and anti-inflammatory activity.

Keywords: carbamates; cholinesterases inhibition; diarylethenes; docking; synthesis

Check for updates

Academic Editor: Alfonso Zambon

Received: 30 September 2026
Revised: 14 October 2026
Accepted: 20 October 2026
Published: 23 October 2026

Copyright: © 2026 by the authors. Licensee MDPI, Basel, Switzerland. This article is an open access article distributed under the terms and conditions of the Creative Commons Attribution (CC BY) license.

1. Introduction

Evidence for a functional link between the cholinergic and immune systems emerged in the early twentieth century from studies of CNI-1493 in rat models. The anti-inflammatory effects of this compound were found to be mediated indirectly, through its activity in the brain rather than by direct effects on circulating immune cells. Notably, a comparable

response could be elicited by vagotomy, implicating the vagus nerve in the regulation of systemic inflammation [1]. Subsequent studies in animal models demonstrated that CNI-1493 reduced systemic TNF-α production in a dose-dependent manner following endotoxin (lipopolysaccharide, LPS) challenge [2]. The cholinergic anti-inflammatory pathway is a key neuroimmune mechanism that constrains the magnitude of the inflammatory response while preserving the capacity to eliminate harmful stimuli. Acetylcholine (ACh) is its principal neurotransmitter and mediates its effects predominantly through the α7 nicotinic acetylcholine receptor (α7nAChR) and the muscarinic M1 acetylcholine receptor (M1AChR) [3]. Activation of this pathway promotes ACh release and engagement of α7nAChR, triggering intracellular Ca^{2+} signaling and downstream pathways that modulate inflammatory responses, including NF-κB-dependent transcription.

The duration and magnitude of cholinergic signaling are tightly regulated by cholinesterases (ChEs), primarily acetylcholinesterase (AChE) and butyrylcholinesterase (BChE), which hydrolyze ACh into choline and acetate. Pharmacological inhibition of these enzymes can therefore increase ACh availability and has been associated with anti-inflammatory effects across experimental models [4–12]. The capacity for cholinergic signaling is not restricted to neuronal cells. Acetylcholine transferase expression has been detected in myeloid cell populations, indicating that these cells can also synthesize ACh. However, expression of the relevant enzymes and, consequently, ACh production appears to be considerably lower in myeloid cells than in lymphocyte populations [13].

Previously prepared analogs **1H–12H** [14] (Figure 1) as resveratrol-inspired structures, which lack the methoxy substituent present in the newly synthesized compounds **1–12**, were shown to be highly potent and selective BChE inhibitors, with no inhibitory activity against AChE. The most active carbamates were approximately 50-fold more potent BChE inhibitors than the standard rivastigmine. Recent studies of *trans*-resveratrol, a member of the stilbene family, have highlighted its potential involvement in several pathophysiological mechanisms associated with Alzheimer's disease (AD). The introduction of the methoxy group in the present series was undertaken to assess its potential contribution to the biological activity of **1–12**, given the positive effect of the methoxy group observed in previous studies on smaller, related diarylethenes **1′** and **2′** (Figure 1), exactly in the same position as in compound 2′. The aim was to see if the prolongation of the conjugation in **1–12** on the thiophene side of the molecules (in comparison with compound **2′** (Figure 1), increase the potential toward BChE inhibition. As discussed, inhibition of AChE and BChE has been associated with anti-inflammatory activity [4]. In our previous in vitro experiments [15], LPS stimulation induced an increase in ACh production. However, the subsequent degradation of ACh was prevented by treatment with cholinesterase inhibitors, in agreement with the results obtained in the biochemical assays. This preservation of ACh was accompanied by attenuation of the inflammatory response, as shown by reduced TNF-α production. Collectively, those findings indicated that the investigated compounds may modulate the inflammatory response through cholinesterase inhibition. In this work, we prepared new resveratrol-inspired thieno-benzimidazole and thieno-oxazole methoxy derivatives **1–12** to explore how combining the methoxy group with different carbamate groups on the same aryl ring affects both anti-inflammatory and cholinesterase-inhibitory biological activity. This study also aimed to evaluate inhibition selectivity and interpret the experimental results using molecular modeling.

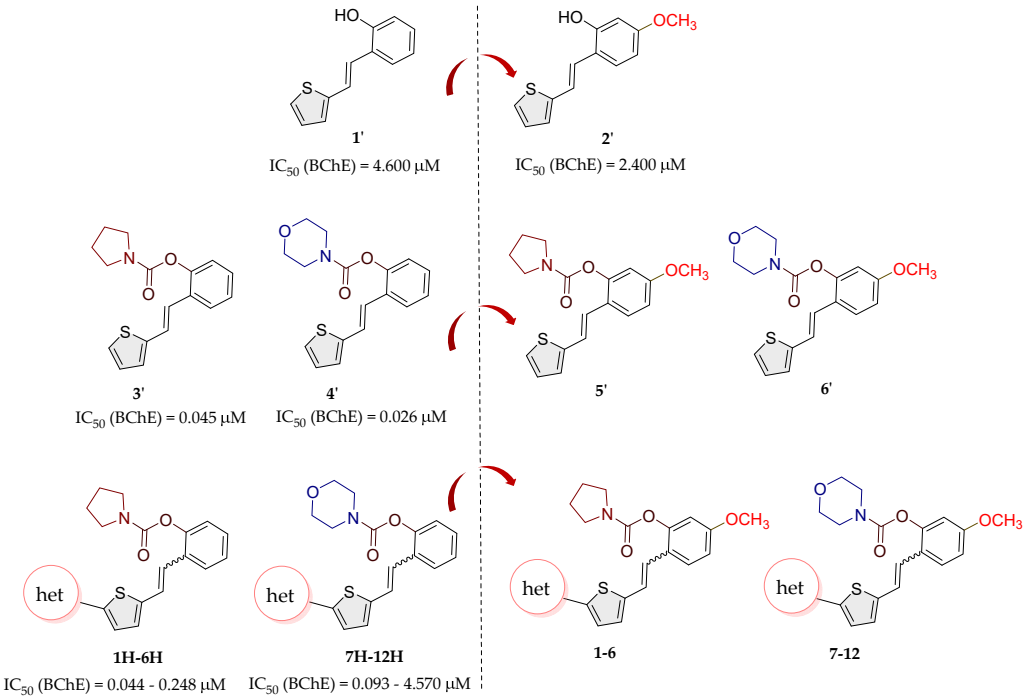


Figure 1. Structures of the first series of explored resveratrol-inspired phenols (**1′** and **2′**), the second (**3′**–**6′**) and the third (**1H**–**12H**) carbamate series as BChE inhibitors.

2. Materials and Methods

2.1. General Remarks

All solvents used in the experimental section were commercially available and were further purified by distillation before use. During extractions, the organic and aqueous layers were separated, and the organic layer was dried over anhydrous magnesium sulfate. Thin-layer chromatography was performed on silica gel-coated aluminum plates (0.2 mm, 60/Kieselguhr F_{254}), detected under UV light at 254 and 366 nm, and chromatographed in 10 mL of the appropriate solvent system. Column chromatography was carried out in glass columns of various diameters packed with silica gel (60 Å, technical grade), with the height of the stationary phase adjusted according to the quantity and nature of the sample. All solvents were removed from the reaction solutions using a rotary evaporator under reduced pressure. Nuclear magnetic resonance (NMR) was used for compound characterization; measurements were performed on a Bruker Avance spectrometer (Billerica, MA, USA) operating at frequencies of 75, 150, and 600 MHz. Samples were prepared by dissolution in deuterated methanol (CD_3OD) and chloroform ($CDCl_3$), using tetramethylsilane (TMS) as an internal standard, which yields a single sharp signal in the spectrum. Chemical shifts are expressed in ppm (parts per million). In the ^1H NMR spectra, alongside the signals of the analyzed compounds, characteristic solvent signals were observed, including residual signals from CD_3OD at approximately 3.2 and 4.8 ppm, and the $CDCl_3$ signal at 7.3 ppm. In the ^{13}C NMR spectrum, a signal for CD_3OD was present at approximately 49 ppm.

2.2. Synthesis of 2-(Bromomethyl)thiophene

Anhydrous diethyl ether (100 mL) was added to a three-necked round-bottom flask, followed by the addition of commercially available 2-thienylmethanol (0.0063 mol). A glass dropping funnel was fitted to the right neck of the flask. A solution of phosphorus tribromide (PBr_3, 0.021 mol) in anhydrous diethyl ether (10 mL) was added dropwise to the reaction mixture under continuous stirring over a period of 15 min. A rapid reaction

was observed during the addition. Upon completion of the addition, the reaction mixture was stirred at room temperature for 1 h.

The reaction was quenched by the addition of a previously prepared water/methanol (100 mL/15 mL) mixture, followed by the addition of an appropriate amount of diethyl ether. The resulting mixture was subjected to extraction, and the organic layer was separated and dried over anhydrous magnesium sulfate ($MgSO_4$). After filtration, the solvent was removed by evaporation to dryness. The resulting 2-(bromomethyl)thiophene was obtained as a yellow oil and used in the subsequent reaction step without further purification.

2.3. Synthesis of the Phosphonium Salt

A total of 50 mL of toluene was added to the 2-(bromomethyl)thiophene, followed by addition of a solution of triphenylphosphine (PPh_3, 0.063 mol) in the same solvent (20 mL). The reaction mixture was stirred at room temperature for four days. Upon completion of the reaction, the mixture was filtered, and the isolated solid product was dried in a desiccator for several days. The isolated product was obtained as a yellowish powder in an amount of 35 g.

2.4. Synthesis of Stilbene Derivatives via the Wittig Reaction

The reaction apparatus, consisting of a two- or three-necked round-bottom flask, a dropping funnel, and a nitrogen or argon gas supply, was purged with the inert gas for approximately 10 min to establish an inert atmosphere. The flask was equipped with a magnetic stir bar and placed on a magnetic stirrer. One of the flask openings was fitted with a calcium chloride ($CaCl_2$) drying tube. Following purging, the dropping funnel was closed, and approximately 100 mL of absolute ethanol, dried over 3 Å molecular sieves, was introduced. The volume of ethanol was adjusted according to the quantities of the starting materials. Approximately 10 mL of the solvent was retained in the dropping funnel, while the remainder was transferred to the reaction flask. The weighed thiophene-based phosphonium salt was then added to the flask, and the mixture was thoroughly stirred. Previously weighed sodium metal (0.015 mol), handled under petroleum ether, was added to the ethanol retained in the dropping funnel. After the sodium had completely reacted, accompanied by the evolution of hydrogen gas, several drops of the freshly prepared base solution were added to the reaction flask. The aldehyde, dissolved in ethanol, was then introduced into the reaction mixture, followed by the dropwise addition of the remaining base solution. Upon completion of the base addition, the dropping funnel was replaced with a stopper, and the reaction mixture was stirred at room temperature. The progress of the reaction was monitored by thin-layer chromatography (TLC). After completion of the reaction, the mixture was diluted with water and extracted with toluene (3 × 50 mL). The organic layer was separated, dried over anhydrous $MgSO_4$, and concentrated to dryness using a rotary evaporator under reduced pressure. The resulting crude solid product 2′ was purified by column chromatography using an appropriate solvent system. Products **1′**, **3′**, **4′**, and **5′** are described in our previous work [14].

(*E*)-5-Methoxy-2-(2-(thiophen-2-yl)vinyl)phenol (**2′**)

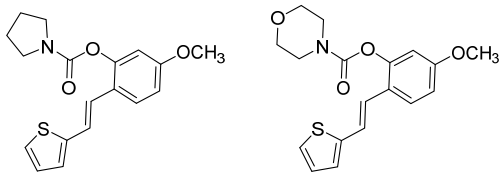
Compound **2′** was synthesized according to the general procedure using 2-hydroxy-4-methoxybenzaldehyde (0.015 mol) and the thiophene-based phosphonium salt (0.015 mol), with sodium metal used in a 10% molar excess (0.015 mol). The total reaction volume was 100 mL. The crude product was purified by column chromatography (column dimensions: d = 2 cm, h = 10 cm) using a petroleum ether/ethyl acetate (PE/EtOAc) mixture (50%/50%). The product was obtained as a white powder (647 mg, 19% isolated yield).

(*E*)-5-Methoxy-2-(2-(thiophen-2-yl)vinyl)phenol (**2′**): 647 mg (isolated yield 19%), R_f (PE/EtOAc, 50%) = 0.89; ^{1}H NMR (600 MHz, CD_3OD) δ/ppm: 7.39 (d, J = 8.6 Hz, 1H), 7.20

(s, 1H), 7.19 (d, J = 5.1 Hz, 1H), 7.16 (d, J = 16.1 Hz, 1H), 7.01 (d, J = 3.4 Hz, 1H), 6.97 (dd, J = 5.0, 3.5 Hz, 1H), 6.44 (dd, J = 8.6, 2.5 Hz, 1H), 6.40 (d, J = 2.5 Hz, 1H), 3.77 (s, 3H).

2.5. Synthesis of Carbamates

The product of the Wittig reaction (300 mg) was dissolved in dichloroethane (DCE) (2.5 mL) in a small round-bottom flask. Triethylamine (TEA, 1.8 equiv) and 4-dimethylaminopyridine (DMAP, 0.087 equiv) were subsequently added to the reaction mixture. The mixture was stirred at room temperature for 15 min under an inert atmosphere, with the reaction vessel briefly purged with argon (up to 1 min) above the surface of the reaction mixture. After 15 min, the appropriate carbamoyl chloride (1.2 equiv) was added dropwise. The reaction mixture was then stirred continuously for 5 h at 60 °C using an oil bath under an inert atmosphere. The progress of the reaction was monitored by thin-layer chromatography (TLC). Upon completion of the reaction, the solvent was removed under reduced pressure using a rotary evaporator. The resulting crude solid was dissolved in dichloromethane (DCM, 10 mL) and transferred to a separatory funnel. The organic phase was washed with distilled water (2 × 10 mL). During the second extraction, the aqueous phase was acidified by the addition of 1 mL of HCl solution (2.4 M). The organic layer was subsequently dried over anhydrous $MgSO_4$ for approximately 15 min, filtered, and concentrated to dryness under reduced pressure using a rotary evaporator. The resulting carbamates **5′** and **6′** were purified by column chromatography using different DCM/PE (0–100%) solvent ratios as the eluent. ^{1}H NMR analysis confirmed that the synthesized carbamates were obtained as the *trans*-isomers.



5' **6'**

(*E*)-5-Methoxy-2-(2-(thiophen-2-yl)vinyl)phenyl-pyrrolidine-1-carboxylate (**5′**)

Pyrrolidine carbamate was synthesized according to the general procedure using (*E*)-5-methoxy-2-(2-(thiophen-2-yl)vinyl)phenol (2′, 0.0011 mol), which was dissolved in DCE (2.5 mL). Triethylamine (TEA, 1.8 equiv, 0.0019 mol), DMAP (0.087 equiv, 0.0009 mol), and pyrrolidine-1-carbonyl chloride (1.2 equiv, 0.0013 mol) were subsequently added. After completion of the reaction and the corresponding extraction procedure, the crude product was purified by column chromatography (column dimensions: d = 2.5 cm, h = 14 cm) using DCM as the eluent.

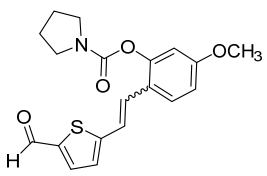
(*E*)-5-Methoxy-2-(2-(thiophen-2-yl)vinyl)phenyl-morpholine-4-carboxylate (**6′**)

Morpholine carbamate was synthesized according to the general procedure using (*E*)-5-methoxy-2-(2-(thiophen-2-yl)vinyl)phenol (2′), which was divided into three identical reaction batches (0.009 mol per batch) and dissolved in DCE (2 mL). To each reaction mixture were added TEA (1.8 equiv, 0.0016 mol), DMAP (0.087 equiv, 0.0008 mol), and morpholine-4-carbonyl chloride (1.2 equiv, 0.0019 mol). Following the extraction procedure, the crude product was purified by column chromatography (column dimensions: d = 2 cm, h = 12 cm) using DCM/PE (70%) as the eluent.

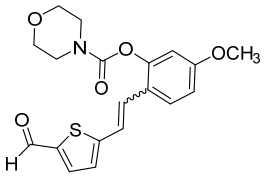
(*E*)-5-Methoxy-2-(2-(thiophen-2-yl)vinyl)phenyl-morpholine-4-carboxylate (**6′**): 589 mg, (isolated yield 62%), R_f (DCM) = 0.75; ^{1}H NMR (600 MHz, CD_3OD) δ/ppm: 7.63 (d, J = 8.7 Hz, 1H), 7.28 (d, J = 5.1 Hz, 1H), 7.23–7.18 (m, 1H), 7.09 (d, J = 3.4 Hz, 1H), 7.02 (dd, J = 5.1, 3.6 Hz, 1H), 6.90–6.84 (m, 2H), 6.72 (d, J = 2.6 Hz, 1H), 3.83 (s, 9H), 3.57 (s, 2H).

2.6. Reaction of Vilsmeier Formylation

The appropriate carbamate was dissolved in an excess of DMF. A portion of the DMF was reserved for preparation of the $POCl_3$/DMF reagent system, while the remaining solvent was used to dissolve the carbamate. In a separate 25 mL flask, $POCl_3$ (5 equiv) was combined with a small amount of DMF. The mixture was cooled to 0 °C in an ice bath. The carbamate solution was then added dropwise to the activated $POCl_3$/DMF system under continuous stirring while maintaining the temperature at 0 °C. The reaction mixture was subsequently stirred at 0 °C for an additional 0.5–1 h. The flask was then removed from the ice bath, and the reaction mixture was stirred at room temperature for an additional 12–24 h, depending on the degree of conversion. Reaction progress was monitored using thin-layer chromatography (TLC). Upon completion of the reaction, the mixture was carefully neutralized with 10% aqueous NaOH. Ice was added during the neutralization to control the exothermic nature of the process. After the mixture had reached room temperature, the aqueous phase was extracted with diethyl ether (3 × 25 mL). The combined organic phases were dried over anhydrous $MgSO_4$, filtered, and concentrated under reduced pressure to afford the crude formylated product. The crude product was subsequently purified by column chromatography. NMR analysis confirmed that the isolated material consisted of a mixture of the corresponding isomers.



5''



6''

2-(2-(5-Formylthiophen-2-yl)vinyl)-5-methoxyphenyl-pyrrolidine-1-carboxylate (**5′′**)

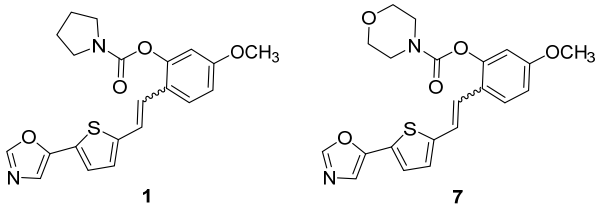
Pyrrolidine carboxylate was synthesized according to the general Vilsmeier formylation procedure using (*E*)-5-methoxy-2-(2-(thiophen-2-yl)vinyl)phenyl pyrrolidine-1-carboxylate (0.006 mol). The starting material was dissolved in an excess of DMF. A portion of the DMF was used to prepare the activated $POCl_3$/DMF system by adding $POCl_3$ (5 equiv), while the remaining DMF was used to dissolve the carbamate. After completion of the reaction and subsequent extraction, the crude product was purified by column chromatography (column dimensions: d = 3 cm, h = 12 cm) using EtOAc as the eluent. The isolated product was then divided into six equal portions to prepare the corresponding final products. The product was obtained in an amount of 171 mg (86% isolated yield) as a mixture of isomers. According to 1H NMR analysis, the trans:cis ratio was 2:1.

2-(2-(5-Formylthiophen-2-yl)vinyl)-5-methoxyphenyl-morpholine-4-carboxylate (**6′′**)

Morpholine carboxylate was synthesized according to the general Vilsmeier formylation procedure using (*E*)-5-methoxy-2-(2-(thiophen-2-yl)vinyl)phenyl-morpholine-4-carboxylate, which was divided into three identical reaction batches (0.006 mol per batch). Each portion was dissolved in an excess of DMF. A portion of the DMF was used to prepare the activated $POCl_3$/DMF system using $POCl_3$ (5 equiv), while the remaining DMF was used to dissolve the carbamate. Following the extraction procedure, the crude product was purified by column chromatography (column dimensions: d = 2 cm, h = 9 cm) using EtOAc/DCM (2%) as the eluent. The isolated product was then divided into six equal portions to prepare the corresponding final products. A total of 276 mg of product was isolated from the three identical reactions, corresponding to a 43% isolated yield of the isomeric mixture. According to ^{1}H NMR analysis, a *trans:cis* ratio of 1:2 was indicated.

2.7. Synthesis of Oxazole Derivatives **1** *and* **7**

The appropriate aldehyde compound was dissolved in methanol (2 mL) in a round-bottom flask equipped with a magnetic stir bar. Upon complete dissolution of the starting material, TosMIC (0.0002 mol) and potassium carbonate (K_2CO_3, 0.0002 mol)) were added to the reaction mixture under continuous stirring. The flask was then closed with a stopper and equipped for reflux by connecting it to a water-cooled condenser fitted with a calcium chloride drying tube. The reaction mixture was heated under reflux in an oil bath at the reflux temperature of methanol for 3 h with continuous stirring, or until complete conversion of the starting aldehyde compound was achieved. The progress of the reaction was monitored through thin-layer chromatography (TLC), when required. After completion of the reaction, the mixture was cooled to room temperature, and methanol was removed under reduced pressure to afford the crude product. The residue was subjected to extraction using ice-cold water and diethyl ether in three consecutive extraction cycles (3 × 25 mL). The combined organic phases were dried over anhydrous $MgSO_4$, filtered, and concentrated under reduced pressure. The resulting crude oxazole derivatives were purified by column chromatography to afford the target compounds. NMR analysis confirmed that the isolated products were obtained as mixtures of the corresponding isomers.



5-Methoxy-2-(2-(5-(oxazol-5-yl)thiophen-2-yl)vinyl)phenyl-pyrrolidine-1-carboxylate (**1**)

Compound **1** was synthesized according to the general procedure using 2-(2-(5-formylthiophen-2-yl)vinyl)-5-methoxyphenyl-pyrrolidine-1-carboxylate (0.0008 mol), which was dissolved in methanol (2 mL). TosMIC (0.0008 mol) and K_2CO_3 (0.0008 mol) were subsequently added to the reaction mixture under continuous stirring. After completion of the reaction and the subsequent extraction procedure, the crude product was purified by column chromatography (column dimensions: d = 1.5 cm, h = 12 cm) using EtOAc/*n*-hexane (60%) as the eluent. The product was obtained as an isomeric mixture (19.4 mg, 60% isolated yield). ^{1}H NMR analysis indicated a trans:cis ratio of 1:0.5. HRMS (ESI) (m/z) for $C_{21}H_{20}N_2O_4S$: $[M + H]^+_{calcd.}$ = 397.1144, $[M + H]^+_{exp.}$ = 397.1215.

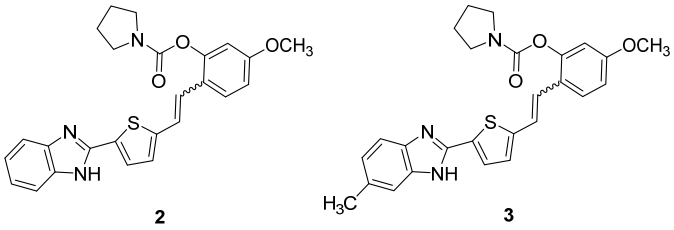
5-Methoxy-2-(2-(5-(oxazol-5-yl)thiophen-2-yl)vinyl)phenyl-morpholine-4-carboxylate (**7**)

Compound **7** was synthesized according to the general procedure using 2-(2-(5-formylthiophen-2-yl)vinyl)-5-methoxyphenyl morpholine-4-carboxylate (0.001 mol), which was dissolved in methanol (2 mL). TosMIC (0.001 mol) and K_2CO_3 (0.001 mol) were subsequently added under continuous stirring. After completion of the reaction and the subsequent extraction procedure, the crude product was purified by column chromatography (column dimensions: d = 2.5 cm, h = 13 cm) using EtOAc/DCM (10%) as the eluent. The product was obtained as an isomeric mixture (7 mg, 13% isolated yield). ^{1}H NMR analysis indicated a *trans:cis* ratio of 1:0.3. HRMS (ESI) (m/z) for $C_{21}H_{20}N_2O_5S$: $[M + H]^+_{calcd.}$ = 412.1093, $[M + H]^+_{exp.}$ = 300.0751 [100%], 437.2019 [10%].

2.8. Synthesis of Benzimidazole Derivatives **2**–**6** *and* **8**–**12**

The appropriate aldehyde derivative was dissolved in absolute ethanol in a small round-bottom flask. The flask was closed with a stopper after addition of the solvent to minimize solvent evaporation. Upon complete dissolution of the substrate under contin-

uous stirring, the appropriate o-phenylenediamine and *p*-benzoquinone were added to the reaction mixture. The reaction flask was subsequently equipped for reflux using a water-cooled condenser and immersed in an oil bath maintained at approximately 110 °C. The reaction mixture was heated under reflux for approximately 1–3 h with continuous stirring, or until satisfactory conversion was achieved. Reaction progress was monitored through thin-layer chromatography (TLC), when required. Upon completion of the reaction, the flask was removed from the oil bath, and the reaction mixture was allowed to cool to room temperature. Ethanol was then removed under reduced pressure to afford the crude benzimidazole derivative. The crude product was subsequently purified by column chromatography. NMR analysis indicated that most synthesized compounds were obtained as *trans*-isomers, whereas only a limited number of derivatives were obtained with a significant proportion of the corresponding *cis*-isomers.



2-(2-(5-(1*H*-Benzo[*d*]imidazol-2-yl)thiophen-2-yl)vinyl)-5-methoxyphenyl-pyrrolidine-1-carboxylate (**2**)

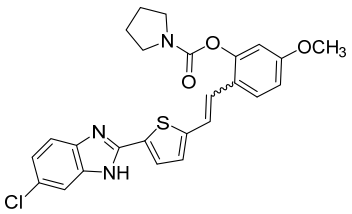
Compound **2** was synthesized according to the general procedure using 2-(2-(5-formylthiophen-2-yl)vinyl)-5-methoxyphenyl-pyrrolidine-1-carboxylate, which was dissolved in absolute ethanol (3 mL). After homogenization of the reaction mixture, benzene-1,2-diamine (0.0008 mol) and *p*-benzoquinone (0.0008 mol) were added. The reaction mixture was heated under reflux in ethanol for 3 h. Upon completion of the reaction, the mixture was allowed to cool to room temperature, and the resulting crude product was purified by column chromatography (column dimensions: d = 1.5 cm, h = 13 cm) using ethyl acetate as the eluent. The product was obtained as an isomeric mixture (15 mg, 42% isolated yield). ^{1}H NMR analysis indicated a *trans:cis* ratio of approximately 1:1. HRMS (ESI) (m/z) for $C_{25}H_{23}N_3O_3S$: $[M + H]^+_{calcd.}$ = 446.1460, $[M + H]^+_{exp.}$ = 446.1527.

2-(2-(5-(6-Methyl-1*H*-benzo[*d*]imidazol-2-yl)thiophen-2-yl)vinyl)-5- methoxyphenyl-pyrrolidine-1-carboxylate (**3**)

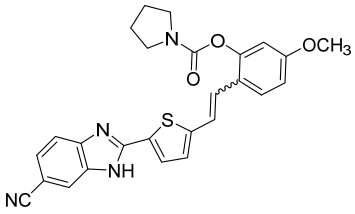
Compound **3** was synthesized according to the general procedure using 2-(2-(5-formylthiophen-2-yl)vinyl)-5-methoxyphenyl pyrrolidine-1-carboxylate, which was dissolved in absolute ethanol (3 mL). 4-Methylbenzene-1,2-diamine (0.0008 mol) and *p*-benzoquinone (8.8 mg, 0.0008 mol) were subsequently added to the reaction mixture. The reaction mixture was heated under reflux for 3 h. After completion of the reaction, the crude product was purified by column chromatography (column dimensions: d = 1.5 cm, h = 13 cm) using EtOAc as the eluent. Further purification was performed by preparative thin-layer chromatography to afford the final product in the required purity. The product was obtained as an isomeric mixture (4.1 mg, 11% isolated yield). ^{1}H NMR analysis indicated a *trans:cis* ratio of 1:0.1. HRMS (ESI) (m/z) for $C_{26}H_{25}N_3O_3S$: $[M + H]^+_{calcd.}$ = 460.1617, $[M + H]^+_{exp.}$ = 460.1674.

(*E*)-2-(2-(5-(6-Methyl-1*H*-benzo[*d*]imidazol-2-yl)thiophen-2-yl)vinyl)-5-methoxyphenyl-pyrrolidine-1-carboxylate (**3**): ^{1}H NMR (600 MHz, CD_3OD) δ/ppm: 7.64 (d, J = 8.7 Hz, 1H), 7.61 (d, J = 3.8 Hz, 1H), 7.38 (m, 2H), 7.22 (d, J = 16.1 Hz, 1H), 7.12 (d, J = 3.8 Hz, 1H), 7.09 (d, J = 8.2 Hz, 1H), 7.07–7.02 (m, 1H), 6.84 (dd, J = 8.7, 2.5 Hz, 1H), 6.75 (d, J = 2.6 Hz, 1H), 3.82 (s, 3H), 3.73 (t, J = 6.8 Hz, 2H), 3.50 (t, J = 6.8 Hz, 2H), 2.45 (s, 3H), 2.11 (m, 2H), 2.03

(m, 2H); ^{13}C NMR (75 MHz, CD_3OD) δ (ppm): 161.8, 154.7, 151.0, 147.3, 132.0, 130.6, 128.5, 128.2, 127.9, 125.4, 124.0, 123.4, 122.2, 113.6, 113.0, 110.0, 109.6, 56.1, 26.9, 25.9, 21.7.



4



5

2-(2-(5-(6-Chloro-1*H*-benzo[*d*]imidazol-2-yl)thiophen-2-yl)vinyl)-5-methoxyphenyl-pyrrolidine-1-carboxylate (**4**)

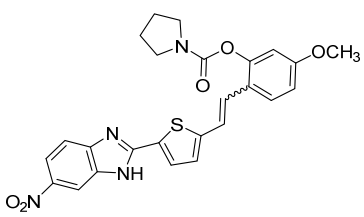
Compound **4** was synthesized according to the general procedure for benzimidazole synthesis, starting from 2-(2-(5-formylthiophen-2-yl)vinyl)-5-methoxyphenyl pyrrolidine-1-carboxylate, which was dissolved in 3 mL of absolute ethanol. After homogenization of the reaction mixture, 4-chlorobenzene-1,2-diamine (0.0008 mol) and *p*-benzoquinone (0.0008 mol) were added. The reaction mixture was then heated under reflux in ethanol for 3 h. After completion of the reaction and cooling to room temperature, the crude product was purified by column chromatography (column dimensions: d = 1.5 cm, h = 12 cm; system E). The product was obtained as an isomeric mixture (21 mg, 55% isolated yield). ^{1}H NMR analysis indicated a *trans:cis* ratio of 1:0.1. HRMS (ESI) (m/z) for $C_{25}H_{22}ClN_3O_3S$: $[M + H]^+_{calcd.}$ = 480.1070, $[M + H]^+_{exp.}$ = 480.1142.

(*E*)-2-(2-(5-(6-Chloro-1*H*-benzo[*d*]imidazol-2-yl)thiophen-2-yl)vinyl)-5-methoxyphenyl-pyrrolidine-1-carboxylate (**4**): ^{1}H NMR (CD_3OD, 600 MHz) δ/ppm: 7.68–7.65 (m, 2H), 7.63–7.42 (m, 2H), 7.24 (m, 2H), 7.16 (d, J = 3.9 Hz, 1H), 7.08 (d, J = 16.2 Hz, 1H), 6.86 (dd, J = 8.9, 2.8 Hz, 1H), 6.76 (d, J = 2.5 Hz, 1H), 3.83 (s, 3H), 3.75 (t, J = 6.8 Hz, 2H), 3.53–3.50 (m, 2H), 2.17–2.08 (m, 2H), 2.08–2.01 (m, 2H); ^{13}C NMR (CD_3OD, 150 MHz) δ/ppm: 160.4, 153.3, 149.6, 148.4, 146.7, 129.8, 129.2, 128.1, 127.9, 126.8, 126.5, 123.0, 121.8, 120.5, 112.1, 108.6, 108.2, 54.7, 29.5, 25.5, 24.6.

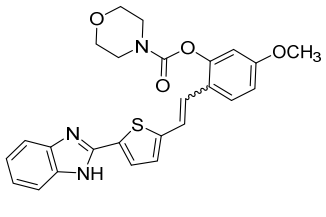
2-(2-(5-(6-Cyano-1*H*-benzo[*d*]imidazol-2-yl)thiophen-2-yl)vinyl)-5-methoxyphenyl-pyrrolidine-1-carboxylate (**5**)

Compound **5** was synthesized according to the general procedure, starting from 2-(2-(5-formylthiophen-2-yl)vinyl)-5-methoxyphenyl pyrrolidine-1-carboxylate, which was dissolved in 3 mL of absolute ethanol. After homogenization of the reaction mixture, 4-cyanobenzene-1,2-diamine (10.8 mg, 0.0008 mol) and *p*-benzoquinone (0.0008 mol) were added. The reaction mixture was heated under reflux in ethanol for 1 h. After completion of the reaction and cooling to room temperature, the crude product was purified by column chromatography (column dimensions: d = 1.5 cm, h = 12 cm; system E). The product was obtained as an isomeric mixture (6.2 mg, 16% isolated yield). ^{1}H NMR analysis indicated a *trans:cis* ratio of 1:8. HRMS (ESI) (m/z) for $C_{26}H_{22}N_4O_3S$: $[M + H]^+_{calcd.}$ = 471.1413, $[M + H]^+_{exp.}$ = 471.1466.

(*Z*)-2-(2-(5-(6-Cyano-1*H*-benzo[*d*]imidazol-2-yl)thiophen-2-yl)vinyl)-5-methoxyphenyl-pyrrolidine-1-carboxylate (**5**): ^{1}H NMR (CD_3OD, 600 MHz) δ/ppm: 8.42 (s, 1H), 8.18 (dd, J = 8.9, 2.2 Hz, 1H), 7.71–7.60 (m, 2H), 7.33 (d, J = 8.4 Hz, 1H), 7.13 (d, J = 3.9 Hz, 1H), 6.93–6.82 (m, 3H), 6.53 (d, J = 11.9 Hz, 1H), 3.87 (s, 3H), 3.38 (m, 4H), 1.97–1.86 (m, 4H).



6



8

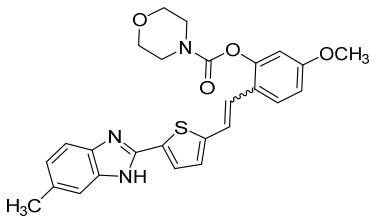
2-(2-(5-(6-Nitro-1*H*-benzo[*d*]imidazol-2-yl)thiophen-2-yl)vinyl)-5-methoxyphenyl-pyrrolidine-1-carboxylate (**6**)

Compound **6** was synthesized according to the general procedure for benzimidazole synthesis, starting from 2-(2-(5-formylthiophen-2-yl)vinyl)-5-methoxyphenyl pyrrolidine-1-carboxylate, which was dissolved in 3 mL of absolute ethanol. After a homogeneous solution had been obtained, 4-nitrobenzene-1,2-diamine (0.0008 mol) and *p*-benzoquinone (0.0008 mol) were added to the reaction mixture.

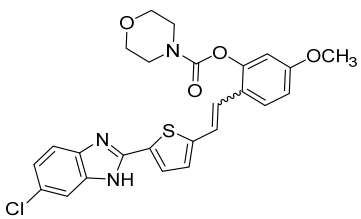
The reaction mixture was then heated under reflux in ethanol for 1 h. After completion of the reaction, the mixture was cooled to room temperature, and the crude product was purified by column chromatography (column dimensions: d = 1.5 cm, h = 12 cm; system E). The product was obtained as an isomeric mixture (26.1 mg, 66% isolated yield). ^{1}H NMR analysis indicated a *trans:cis* ratio of 1:1.7. HRMS (ESI) (m/z) for $C_{25}H_{22}N_4O_5S$: $[M + H]^+_{calcd.}$ = 491.1311, $[M + H]^+_{exp.}$ = 491.1366.

2-(2-(5-(1*H*-Benzo[*d*]imidazol-2-yl)thiophen-2-yl)vinyl)-5-methoxyphenyl morpholine-4-carboxylate (**8**)

Compound **8** was synthesized according to the general procedure, starting from 2-(2-(5-formylthiophen-2-yl)vinyl)-5-methoxyphenyl morpholine-4-carboxylate, which was dissolved in 3 mL of absolute ethanol. After a homogeneous solution had been obtained, benzene-1,2-diamine (0.001 mol) and *p*-benzoquinone (0.001 mol) were added to the reaction mixture. The reaction mixture was then heated under reflux in ethanol for 3 h. After completion of the reaction, the mixture was cooled to room temperature, and the crude product was purified by column chromatography (column dimensions: d = 2 cm, h = 13 cm; system E). The product was obtained as an isomeric mixture (1.8 mg, 8% isolated yield). ^{1}H NMR analysis indicated a *trans:cis* ratio of 1:1.5. HRMS (ESI) (m/z) for $C_{25}H_{23}N_3O_4S$: $[M + H]^+_{calcd.}$ = 462.1409, $[M + H]^+_{exp.}$ = 462.1484.



9



10

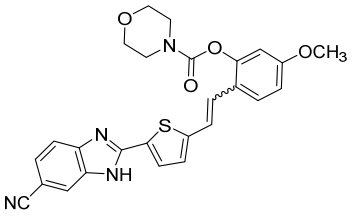
2-(2-(5-(6-Methyl-1*H*-benzo[*d*]imidazol-2-yl)thiophen-2-yl)vinyl)-5-methoxyphenyl morpholine-4-carboxylate (**9**)

Compound **9** was synthesized using the general procedure for benzimidazole synthesis, starting from 2-(2-(5-formylthiophen-2-yl)vinyl)-5-methoxyphenyl morpholine-4-carboxylate, which was dissolved in 3 mL of absolute ethanol. After a homogeneous solution had been obtained, 4-methylbenzene-1,2-diamine (0.001 mol) and *p*-benzoquinone (0.001 mol) were added to the reaction mixture. The reaction mixture was then heated under reflux in ethanol for 3 h. After completion of the reaction, the mixture was cooled to room temperature, and the crude product was purified by column chromatography (column dimensions: d =

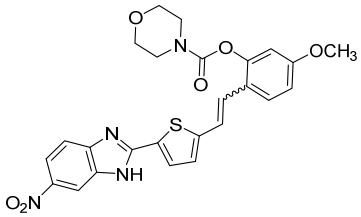
3 cm, *h* = 11 cm; system E). The product was obtained as an isomeric mixture (8.3 mg, 14% isolated yield). ^{1}H NMR analysis indicated a *trans:cis* ratio of 1:0.4. HRMS (ESI) (*m*/*z*) for $C_{26}H_{25}N_3O_4S$: $[M + H]^+_{calcd.}$ = 476.1566, $[M + H]^+_{exp.}$ = 476.1648.

2-(2-(5-(6-Chloro-1*H*-benzo[*d*]imidazol-2-yl)thiophen-2-yl)vinyl)-5-methoxyphenyl-morpholine-4-carboxylate (**10**)

Compound **10** was synthesized according to the general procedure, starting from 2-(2-(5-formylthiophen-2-yl)vinyl)-5-methoxyphenyl morpholine-4-carboxylate, which was dissolved in 3 mL of absolute ethanol. After homogenization of the reaction mixture, 4-chlorobenzene-1,2-diamine (0.001 mol) and *p*-benzoquinone (0.001 mol) were added. The reaction mixture was heated under reflux in ethanol for 3 h. After completion of the reaction and cooling to room temperature, the crude product was purified by column chromatography (column dimensions: *d* = 3 cm, *h* = 13 cm; system E). Additional purification was performed by preparative thin-layer chromatography to obtain the final product of the required purity. The product was obtained as an isomeric mixture (7.2 mg, 12% isolated yield). ^{1}H NMR analysis indicated a *trans:cis* ratio of 1:0.6. HRMS (ESI) (*m*/*z*) for $C_{25}H_{22}ClN_3O_4S$: $[M + H]^+_{calcd.}$ = 496.1020, $[M + H]^+_{exp.}$ = 518.0928 [100%], 496.1109 [50%].



11



12

2-(2-(5-(6-Cyano-1*H*-benzo[*d*]imidazol-2-yl)thiophen-2-yl)vinyl)-5-methoxyphenyl morpholine-4-carboxylate (**11**)

Compound **11** was synthesized according to the general procedure, starting from 2-(2-(5-formylthiophen-2-yl)vinyl)-5-methoxyphenyl morpholine-4-carboxylate, which was dissolved in 3 mL of absolute ethanol. After homogenization of the reaction mixture, 4-cyanobenzene-1,2-diamine (16.8 mg, 0.001 mol) and *p*-benzoquinone (0.001 mol) were added. The reaction mixture was heated under reflux in ethanol for 1 h. After completion of the reaction and cooling to room temperature, the crude product was purified by column chromatography (column dimensions: *d* = 2.5 cm, *h* = 12 cm; system E). The product was obtained as an isomeric mixture (19.8 mg, 32% isolated yield). ^{1}H NMR analysis indicated a *trans:cis* ratio of 1:9. HRMS (ESI) (*m*/*z*) for $C_{26}H_{22}N_4O_4S$: $[M + H]^+_{calcd.}$ = 487.1362, $[M + H]^+_{exp.}$ = 487.1439.

(*Z*)-2-(2-(5-(6-Cyano-1*H*-benzo[*d*]imidazol-2-yl)thiophen-2-yl)vinyl)-5-methoxyphenyl morpholine-4-carboxylate (**11**): ^{1}H NMR (CD_3OD, 600 MHz) δ/ppm: 7.60 (d, *J* = 8.7 Hz, 3H), 7.32–7.30 (m, 1H), 7.13 (d, *J* = 3.9 Hz, 1H), 6.94 (d, *J* = 0.8 Hz, 1H), 6.91 (dd, *J* = 8.5, 2.6 Hz, 1H), 6.90–6.87 (m, 1H), 6.83 (d, *J* = 2.5 Hz, 1H), 6.50 (d, *J* = 11.7 Hz, 1H), 3.87 (s, 4H), 3.64–3.60 (m, 4H), 3.46 (s, 3H).

2-(2-(5-(6-Nitro-1*H*-benzo[*d*]imidazol-2-yl)thiophen-2-yl)vinyl)-5-methoxyphenyl-morpholine-4-carboxylate (**12**)

Compound **12** was synthesized according to the general procedure for benzimidazole synthesis, starting from 2-(2-(5-formylthiophen-2-yl)vinyl)-5-methoxyphenyl morpholine-4-carboxylate, which was dissolved in 3 mL of absolute ethanol. After a homogeneous solution had been obtained, 4-nitrobenzene-1,2-diamine (0.001 mmol) and *p*-benzoquinone (0.001 mol) were added to the reaction mixture. The reaction mixture was then heated under reflux in ethanol for 1 h. After completion of the reaction, the mixture was cooled to room

temperature, and the crude product was purified by column chromatography (column dimensions: d = 1.5 cm, h = 12 cm; system E). Additional purification was performed by preparative thin-layer chromatography to obtain the final product of the required purity. The product was obtained as an isomeric mixture (9.5 mg, 1% isolated yield). ^{1}H NMR analysis indicated a *trans:cis* ratio of 1:0.1. HRMS (ESI) (m/z) for $C_{25}H_{22}N_4O_6S$: [M + H]$^+_{calcd.}$ = 506.1260, [M + H]$^+_{exp.}$ = 537.3946 [100%], 437.1936 [10%].

(*E*)-2-(2-(5-(6-Nitro-1*H*-benzo[*d*]imidazol-2-yl)thiophen-2-yl)vinyl)-5-methoxyphenyl-morpholine-4-carboxylate (**12**): ^{1}H NMR (CD_3OD, 600 MHz) δ/ppm: 8.22 (dd, J = 8.8, 2.2 Hz, 1H), 7.78 (d, J = 3.8 Hz, 1H), 7.70 (d, J = 8.7 Hz, 2H), 7.29 (d, J = 16.0 Hz, 1H), 7.24 (d, J = 3.9 Hz, 1H), 7.09 (d, J = 16.1 Hz, 1H), 6.92–6.89 (m, 1H), 6.76 (m, 1H), 3.85 (s, 12H).

2.9. In Vitro ChE Activity Assay

Reagents were purchased from Sigma-Aldrich (St. Louis, MO, USA) as follows: acetylcholinesterase from electric eel (eeAChE, type VI-S), butyrylcholinesterase from horse serum (eqBChE), acetylthiocholine iodide (ATChI), S-butyrylthiocholine iodide (BTChI), Tris base, 96% ethanol, and 5,5′-dithiobis-(2-nitrobenzoic acid) (DTNB). Rivastigmine was obtained from BLD Pharmatech Ltd. (Hiderabad, India).

Cholinesterase activity was measured using a modified Ellman method [16] at room temperature with a 96-well microplate reader (Agilent, BioTek 800TS, (BioTek Instruments, Winooski, VT, USA)). The inhibition mixture contained 180 µL of Tris buffer (50 mM, pH 8.0), 10 µL of AChE or BChE enzyme (prepared in 20 mM Tris buffer, pH 7.5; final concentration 0.66 U/mL), 10 µL of DTNB (final concentration 0.3 mM), and 10 µL of sample dissolved in ethanol (final concentrations ranging from 0.01 to 25 µM). Incubation of the novel resveratrol-inspired methoxy carbamates with cholinesterases lasted 30 min, after which the reaction was initiated by adding the substrate ATChI/BTChI (10 µL, final concentration 0.5 mM). Following a four-minute reaction time, absorbance was recorded at 405 nm.

All assays were conducted in triplicate, with the remaining enzyme activity expressed as the mean ± standard deviation (SD). IC_{50} values were determined by nonlinear regression of mean activity values (±standard deviation) against the logarithm of compound concentration.

2.10. Anti-Inflammatory Activity

Human peripheral blood mononuclear cells (PBMCs) were isolated from healthy volunteers' buffy coats and treated as previously described [15]. Briefly, 200,000 cells/well were seeded in 96-well plates in RPMI 1640 medium (Lonza, Gampel, Switzerland) supplemented with 10% FBS (Biowest, Nuaillé, France). Compounds were tested in duplicate across a concentration range of 100 µM to 0.046 µM, using 3-fold serial dilutions, while dexamethasone was tested from 1 µM to 0.46 nM, also using 3-fold serial dilutions. 0.1% DMSO was used as a vehicle control. After 1 h pre-incubation at 37 °C, 5% CO_2, and 95% humidity, cells were stimulated with 1 ng/mL LPS for 24 h. After 24 h incubation, cell viability was assessed from the cells using CellTiter-Glo (Promega, Madison, WI, USA), as previously described [15], while supernatants were collected for TNFα quantification.

Enzyme-linked immunosorbent assay (ELISA). TNFα levels were measured using 384-well sandwich ELISA, as previously described [15]. Briefly, lumitrac 600 microplates (Greiner Bio-One, Kremsmünster, Austria) were coated with 1 µg/mL of TNFα capture antibody (BD Pharmingen, San Jose, CA, USA) and incubated overnight at 4 ∘C. Plates were blocked using 1% BSA (Sigma-Aldrich, Burlington, MA, USA) and 5% sucrose (Kemika, Zagreb, Croatia) in PBS (Gibco, Miami, FL, USA), after which standard or undiluted supernatants were added. Following overnight incubation, 250 ng/mL TNFα detection antibody (BD Pharmingen, USA) was added and incubated for 2 h at room temperature

(RT). Plates were then incubated with 500 ng/mL Streptavidin-HRP (Invitrogen, Carlsbad, CA, USA) for 45 min at RT before chemiluminescence ELISA substrate (Roche, Basel, Switzerland) addition. Luminescence was measured using EnVision 2105 Multilabel Plate Reader (Perkin Elmer, Waltham, MA, USA).

Data analysis. TNFα concentrations were interpolated from a standard curve after blank subtraction. Percentages of inhibition of each compound were calculated from the obtained cytokine concentrations using the formula: % of inhibition = 100 − (((compound − no trigger)/(trigger − no trigger)) × 100). For viability assessment, luminescence values were normalized to the trigger control. Concentrations reducing cell viability ≥20% were considered cytotoxic and were excluded from further IC_{50} calculation. All calculations were performed using Microsoft Excel software, and IC_{50} values were determined in GraphPad Prism 9.

2.11. Computational Details

The geometries of the two selected ligands were optimized at the M06-2X/6-31G(d) level of theory using the Gaussian program package [17] and then used as input structures for molecular docking calculations. Docking was performed with AutoDock 4.2 [18] using the crystal structure of human butyrylcholinesterase (PDB ID: 1P0I [19]). Human BChE was selected for molecular docking because an experimentally determined structure of equine BChE is currently unavailable. The use of human BChE as a structural model is supported by the high sequence similarity between the two enzymes (approximately 90%) and the complete conservation of the 14 key amino acid residues forming the active-site gorge [20]. Before docking, polar hydrogen atoms were added to the receptor, and Kollman partial charges were assigned, whereas Gasteiger charges were used for the ligands. The receptor was kept rigid throughout the docking calculations, while ligand conformational flexibility was retained. The docking search was carried out using the Lamarckian genetic algorithm (LGA). The search space was defined by a grid box of 60 × 72 × 60 points with a grid spacing of 0.375 Å, centered on the BChE active-site gorge to encompass the catalytic site and the surrounding substrate-binding subsites. For each ligand, 50 independent docking runs were performed using a population size of 200 individuals, with a maximum of 25,000,000 energy evaluations and 27,000 generations per run. The mutation and crossover rates were set to 0.02 and 0.80, respectively, with an elitism value of 1. Local optimization was performed using the pseudo-Solis and Wets algorithm.

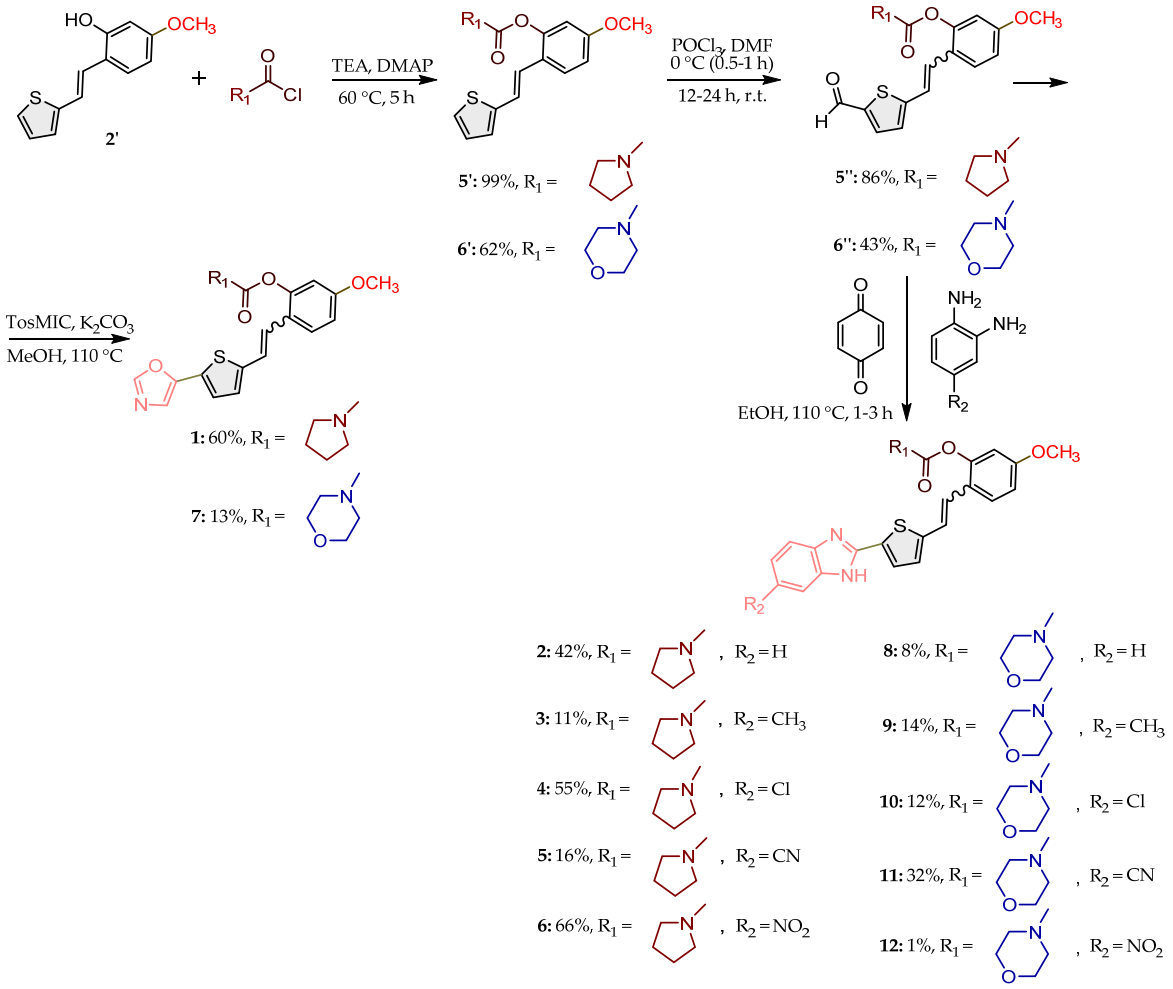
The resulting docking poses were ranked according to the AutoDock estimated binding energy and clustered using an RMSD tolerance of 2.0 Å. Representative conformations from the most populated and energetically favorable clusters were selected for analysis of ligand-enzyme interactions.

3. Results and Discussion

3.1. Synthesis and Characterization of New Methoxy Carbamates **1**–**12**

In this study, we synthesized a series of methoxy-substituted pyrrolidine- and morpholine-based oxazole and benzimidazole carbamates **1**–**12** (Scheme 1) to investigate how the methoxy substituent affects biological activity compared with previously synthesized analogs lacking the methoxy group [14]. The synthetic route involved a sequence of consecutive reactions, beginning with the two-step preparation of thiophene salt from 2-thiophenemethanol, phosphorus bromide, and an appropriate amount of triphenylphosphine by standard laboratory procedures [21,22]. The resulting salt was subsequently employed in a Wittig reaction with 2-hydroxy-4-methoxybenzaldehyde, affording the *trans*-thienostilbene derivative **2′** (Scheme 1) besides a small amount of the corresponding *cis*-isomer. Next, the pyrrolidine and morpholine carbamates **5′** and **6′** (as pure *trans*-

isomers, Scheme 1) were prepared from 2′ (as pure *trans*-isomer) by its reaction with the corresponding carbamoyl chlorides in the presence of TEA and DMAP. The resulting carbamates were then subjected to Vilsmeier formylation using excess DMF and $POCl_3$, yielding the corresponding aldehydes **5″** and **6″** (as the pure *trans* isomer for **5″**, and as a mixture of isomers, *trans:cis* = 1:2, for **6″**).



Scheme 1. Synthetic pathway for obtaining the targeted methoxy-substituted pyrrolidine- and morpholine-based oxazole and benzimidazole carbamates **8**–**12**.

Finally, the aldehydes **5″** and **6″** were converted into two groups of compounds: pyrrolidine (**1**–**6**, isolated yields 11–66%) and morpholine (**7**–**12**, isolated yields 1–32%) derivatives bearing oxazole or benzimidazole subunits (Figure 1). These heterocyclic cores attached to a thiophene ring in new compounds **1**–**12**, in addition to representing target structures for testing cholinesterase inhibition and anti-inflammatory activity, ensure extended conjugation and a bathochromic shift in UV/Vis spectra in comparison with the intermediate carbamates **5′** and **6′** as demonstrated earlier by examples of analogs lacking the methoxy group (Figure 1) [14]. New oxazole derivatives **1** and **7** were obtained by reaction with TosMIC in the presence of potassium carbonate. This procedure afforded the pyrrolidine oxazole **1** and morpholine oxazole **7**. The benzimidazole derivatives **2**–**6** and **8**–**12** were synthesized by reaction of the corresponding aldehydes **5″** and **6″** with the appropriate diamines and *p*-benzoquinone. This approach afforded pyrrolidine benzimidazoles **2**–**6** and morpholine benzimidazoles **8**–**12** (Scheme 1).

UV–Vis spectra of benzimidazole and oxazole derivatives of morpholine and pyrrolidine carbamates **1**–**12** (Figure 2) are typical for diarylethenes [23,24] with strong absorption

between 360–400 nm in CH_3CN. Given that the *trans* configuration at the carbon-carbon double bond is preferred across a wide range of resveratrol-inspired structures as well as resveratrol, it is necessary to address the tendency for isomerization at this bond during specific stages of the reaction pathway for this new group of target structures as well. NMR analyses indicated partial isomerization (to *cis*-isomers) in the key last step of the reaction pathway to obtain **1**–**12**, depending primarily on the substituents. Products **1**–**12** were all isolated as isomer mixtures (with different isomer ratios) and could not be separated due to their very similar polarities, despite repeated attempts by column chromatography. The compositions of the reaction mixtures (according to NMR analysis), with precise isomer ratios obtained after successive column chromatography steps are the following (*trans:cis*): **1** (1:0.5), **2** (1:1), **3** (1:0.1), **4** (1:0.1), **5** (1:8), **6** (1:1.7), **7** (1:0.3), **8** (1:1), **9** (1:0.4), **10** (1:0.6), **11** (1:9), **12** (1:0.1); and they were used for both qualitative UV spectral analysis and biological assays. This factor must be taken into account when interpreting all the results. It is interesting to note that the pyrrolidine derivatives exhibit a bathochromic shift relative to the morpholine analogs (Figure 2, left). In contrast, no such shift is observed when comparing them to the corresponding carbamates lacking the methoxy group, except for the cyano derivative **11**, particularly given the 90% *cis*-isomer content in the isomer mixture (Figure 2, right).

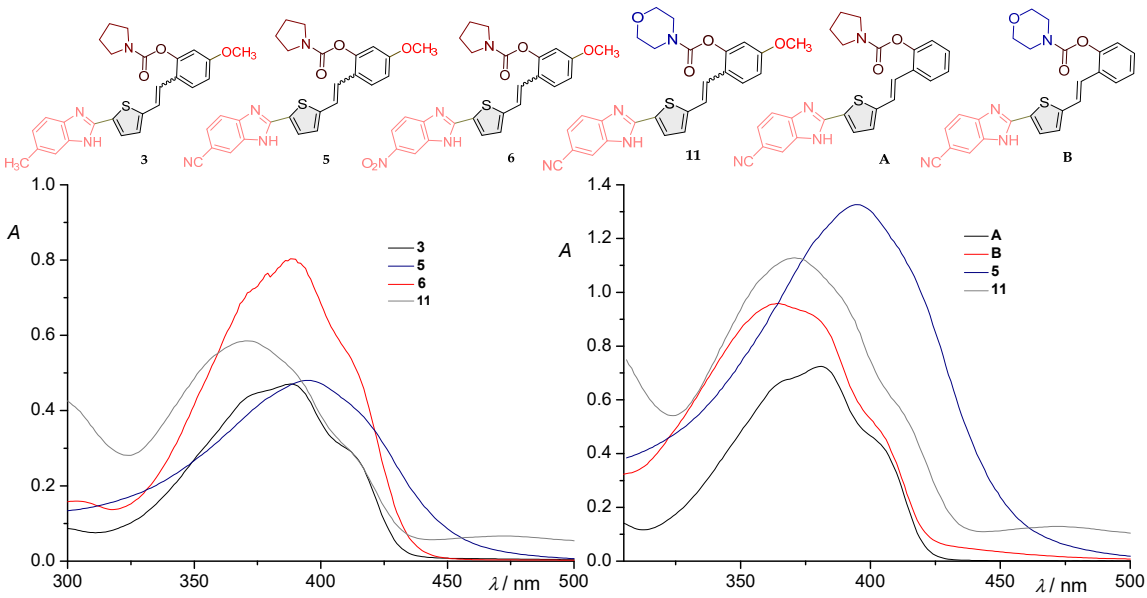


Figure 2. Quantitative UV–Vis spectra (CH_3CN) of different methoxy diarylethene carbamates **3**, **5**, **6** and **11** ((**left**), as mixtures of isomers with different isomer ratio isolated after synthesis) and their comparison with the previous cyano analogs **A** and **B** (CH_3CN) lacking the methoxy group (**right**).

All newly synthesized benzimidazole and oxazole derivatives of morpholine and pyrrolidine carbamates **1**–**12** were characterized spectroscopically, and their structures were confirmed by NMR, MS, and HRMS analyses (Figures S1–S27). In the aliphatic and aromatic parts of the proton spectra of benzimidazole and oxazole carbamates **1**–**12**, the expected number of signals with characteristic coupling constants for aromatic, thiophene, morpholine, and pyrrolidine protons and the trans/cis configuration on the double bond are observed (see Section 2).

3.2. Cholinesterase Inhibition Potential of Methoxy Carbamates **1**–**12**

The inhibitory potential of novel resveratrol-inspired methoxy carbamates **1**–**12** against acetylcholinesterase (eeAChE) and butyrylcholinesterase (eqBChE) was evaluated using a modified Ellman spectrophotometric method. These investigations are a continuation of our previously studied, newly synthesized resveratrol-inspired thieno-benzimidazole and

thieno-oxazole derivatives **1H–12H** (Figure 1) [14], which exhibited potent and selective BChE inhibition (Figure 3). The introduction of a methoxy group into this series (**1–12**) was carried out to assess its potential contribution to biological activity. Rivastigmine, a clinically approved carbamate-based cholinesterase inhibitor, was used as a standard reference compound. Experimental results, expressed as IC_{50} values (μM) and remaining enzyme activity (%) at the maximum tested concentrations, are summarized in Table 1. The maximum tested concentrations for each methoxy carbamate varied as they were tailored to accommodate differences in their specific inhibitory potencies and solubility limits. This adjustment was necessary to prevent microprecipitation under the assay conditions and ensure reliable, artifact-free absorbance measurements.

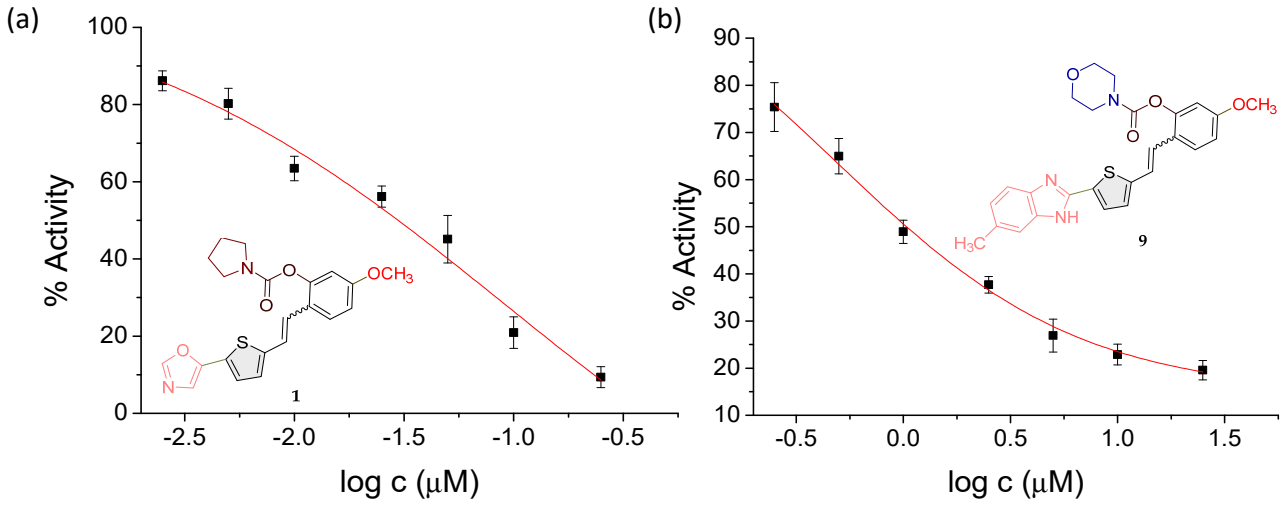


Figure 3. IC_{50} curves of BChE in the presence of carbamates **1** (**a**) and **9** (**b**).

Table 1. Activity of eeAChE and eqBChE in the presence of carbamates **1–12**, and calculated IC_{50} values.

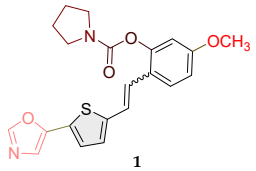
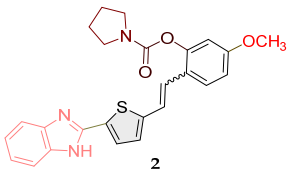
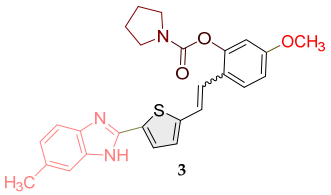
Compound	AChE		BChE	
	% Activity *	IC_{50}/μM	% Activity *	IC_{50}/μM
 **1**	73.5 ± 4.3 (10)	-	9.3 ± 2.7 (0.25)	0.09
 **2**	72.0 ± 2.9 (5)	-	3.5 ± 1.1 (5)	0.24
 **3**	65.0 ± 5.9 (2.5)	-	20.0 ± 4.3 (5)	0.37

Table 1. *Cont.*

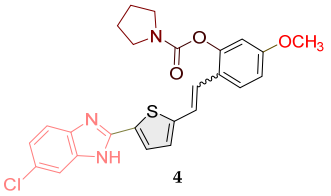
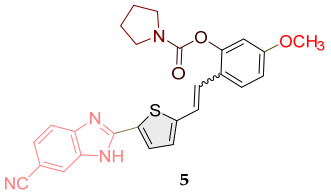
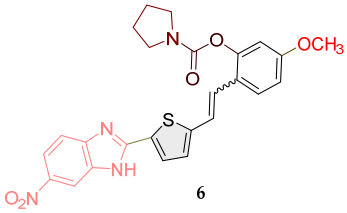
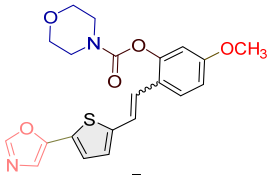
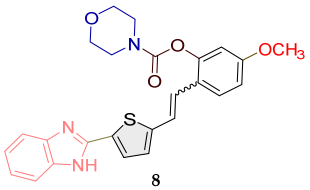
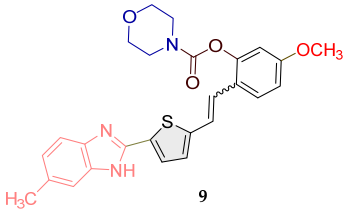
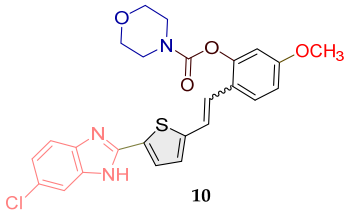
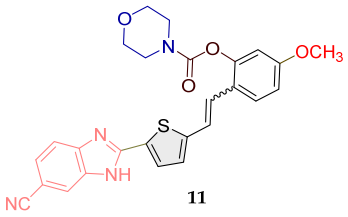
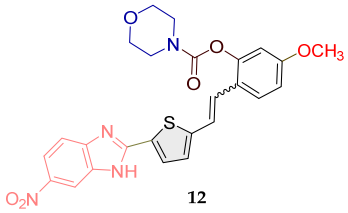
Compound	AChE		BChE	
	% Activity *	IC_{50}/μM	% Activity *	IC_{50}/μM
 **4**	71.9 ± 0.6 (10)	-	22.1 ± 2.7 (10)	0.16
 **5**	**	**	**	**
 **6**	32.6 ± 0.4 (2.5)	-	5.2 ± 1.1 (2.5)	0.54
 **7**	70.8 ± 4.5 (10)	-	6.0 ± 0.7 (50)	5.80
 **8**	80.6 ± 3.8 (10)	-	7.7 ± 0.8 (25)	0.80
 **9**	85.8 ± 4.6 (10)	-	19.6 ± 2.0 (25)	0.48
 **10**	**	**	**	**

Table 1. *Cont.*

Compound	AChE		BChE	
	% Activity *	IC_{50}/μM	% Activity *	IC_{50}/μM
 **11**	**	**	**	**
 **12**	78.0 ± 0.6 (25)	-	22.1 ± 2.7 (25)	2.03
Rivastigmine	47.2 ± 0.2 (100)	-	15.9 ± 0.50 (25)	2.23

* Numbers given in parentheses represent maximal concentrations tested in μM. ** Not able to dissolve under experimental conditions.

All tested methoxy carbamates (**1**–**4**, **6**–**9**, and **12**) demonstrated strong selective inhibition of BChE, whereas their inhibitory activity against AChE remained very weak even at the maximum measured concentrations (2.5–25 μM). Compounds **5**, **10**, and **11** could not be dissolved under the testing conditions; consequently, their cholinesterase inhibitory activity could not be determined.

As representative examples for IC_{50} determination, the BChE concentration-response curves for compounds **1** and **9** are presented in Figure 3. The corresponding graphs include the chemical structures of the selected representatives, whereas the curves for the remaining derivatives are provided in the Supplementary Materials. The structure–activity relationships (SARs) of the tested methoxy carbamates can be analyzed in terms of the following features: the type of substituent on the carbamate nitrogen atom (pyrrolidine or morpholine), the heterocyclic ring fused to the thiophene core (oxazole or benzimidazole), the substituent on the benzimidazole ring, and their comparison with precursors lacking the methoxy group (**1H**–**12H**).

A comparison of structurally corresponding pairs revealed that the pyrrolidine-based carbamates (**1**–**4**, **6**) were consistently more potent BChE inhibitors than their morpholine analogs (**7**–**9**, **12**). The pyrrolidine-oxazole derivative **1** (IC_{50} = 0.09 μM) was over 60 times more potent than the morpholine-oxazole analog **7** (IC_{50} = 5.80 μM). Compound **1** is also the most potent BChE inhibitor in the entire series, being approximately 25-fold more potent than the standard drug rivastigmine (IC_{50} = 2.23 μM). Furthermore, the unsubstituted pyrrolidine-benzimidazole **2** (IC_{50} = 0.24 μM) exhibited a threefold higher inhibitory activity compared to the corresponding morpholine derivative **8** (IC_{50} = 0.80 μM)

Within the morpholine series, incorporating the benzimidazole moiety generally enhanced potency compared with the oxazole derivative **7**; specifically, the morpholine-benzimidazole derivatives **9** and **8** showed significant activity, outperforming rivastigmine. In contrast, for the pyrrolidine series, the incorporation of the benzimidazole core did not increase potency relative to the oxazole counterpart.

Substituent variation on the benzimidazole core had differential effects on BChE inhibition across the two sub-series. In the pyrrolidine series, the introduction of a chlorine substituent (**4**) enhanced activity (IC_{50} = 0.16 μM) compared to the unsubstituted analog **2**.

Conversely, the introduction of a methyl group (**3**) or a strongly electron-withdrawing nitro group (**6**) resulted in a moderate decrease in potency. In the morpholine series, introduction of a methyl group in compound **9** increased potency relative to the unsubstituted analog **8**, whereas the nitro derivative **12** was the least potent among the soluble morpholine benzimidazoles, with potency approaching that of rivastigmine.

A comparison of the new series of compounds **1**–**4**, **6**–**9**, and **12** containing the 5-methoxy group with the previously described analogs lacking the methoxy group (**1H**–**12H**) revealed a positive effect only for compound 1 (pyrrolidine-oxazole scaffold) relative to its non-methoxy analog (**1H**, IC_{50} = 0.25 μM) [14]. For most compounds in the benzimidazole series, introducing the 4-methoxy group generally decreased BChE inhibition potency compared with the non-methoxy analogs, which previously exhibited potent nanomolar BChE inhibition. It is important to highlight that compounds **1**–**12** were tested as mixtures of *trans*- and *cis*-isomers. It is well established that *trans*-isomers are superior cholinesterase inhibitors [14] because they adopt the extended conformation required for optimal accommodation within the active-site channel of the enzyme. The presence of varying proportions of the less active *cis*-isomer inevitably diminishes the overall potency of these compounds. Furthermore, the increased steric hindrance of the 5-methoxy group on the central aryl ring may adversely affect the binding orientation within the active site.

The preliminary (Q)SAR assessment revealed differences in the predicted mutagenic potential of the three compounds (**1**, **4**, and **9**), which showed the best biological assessment. Compound **1** was classified as ICH M7(R2) Class 5, with no structural alerts identified by Derek Nexus, whereas compounds **4** and **9** were assigned to Class 3 based on positive Derek Nexus predictions. The latter two compound contain a substituted benzimidazole moiety, which may contribute to the observed structural alerts, although the benzimidazole scaffold itself is not inherently mutagenic. Notably, Sarah Nexus provided a negative prediction for **9**, highlighting the importance of evaluating the structural and mechanistic relevance of the alerts rather than relying solely on individual computational predictions. These findings indicate that relatively minor structural modifications may influence the predicted mutagenic liability and emphasize the need for expert review before establishing a definitive ICH M7 classification.

3.3. Anti-Inflammatory Activity of Methoxy Carbamates **1**–**12**

The potential anti-inflammatory activity of methoxy carbamates was assessed by measuring TNFα production in human peripheral blood mononuclear cells (PBMC) stimulated with lipopolysaccharide (LPS). Among the tested compounds, only methoxy-substituted pyrrolidine-based oxazole carbamate **1** inhibited TNFα production in a concentration-dependent manner, with an average IC_{50} of 4.3 μM across 3 donors (Figure 4). The other tested compounds did not concentration-dependently inhibit TNFα production. Dexamethasone was used as a positive control, with an average IC_{50} value of 8 nM in 3 donors. Methoxy-substituted pyrrolidine-based oxazole carbamate **1** treatment did not affect PBMC cell viability, as shown in Figure 5. Notably, compound 1 shows the best selective inhibition of BChE, which may indicate a link between the cholinergic and immune systems, as described in the Introduction [3].

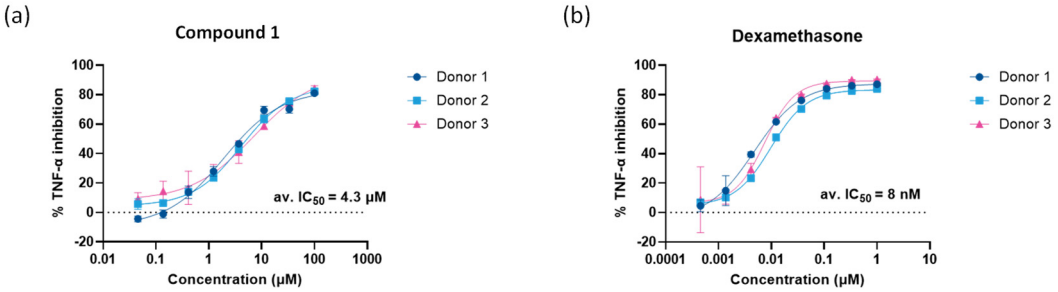


Figure 4. Inhibition of TNFα production in LPS-stimulated PBMCs by the best methoxy-substituted pyrrolidine-based oxazole carbamate **1** (**a**) and dexamethasone (**b**).

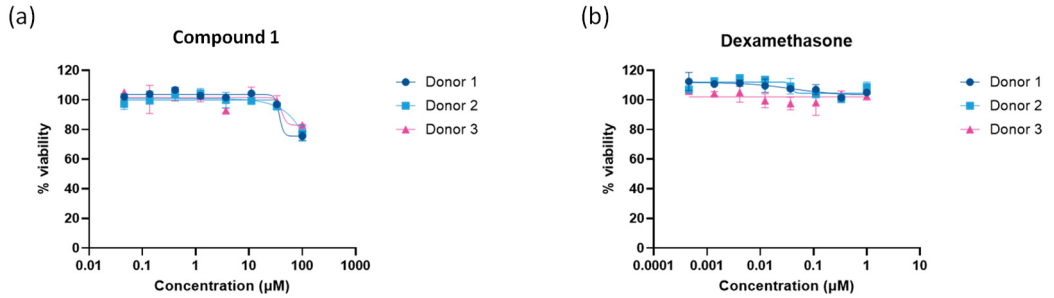


Figure 5. Effect of the best methoxy-substituted pyrrolidine-based oxazole carbamate **1** (**a**) and dexamethasone (**b**) on LPS-stimulated PBMC cell viability after 24 h treatment.

3.4. Molecular Docking of Selected Carbamates

To complement the experimental inhibition data and to examine plausible binding modes of the newly synthesized carbamates within the BChE active-site gorge, molecular docking was performed for two representative ligands, compounds **1** and **9**. We selected these compounds because they represent two structurally distinct members of the series, combining different heteroaromatic systems and carbamate substituents, while both show pronounced inhibitory activity toward BChE. Compound **1** contains an oxazole moiety and a pyrrolidine carbamate, whereas compound **9** contains a methyl-substituted benzimidazole moiety and a morpholine carbamate. The docking analysis was therefore intended primarily to illustrate how these structurally different ligands can be accommodated within the active site and which interactions may contribute to stabilization of the corresponding complexes.

For compound **1**, two closely related docking solutions were obtained with very similar estimated binding energies. The most populated cluster, represented by the pose shown in Figure 6a, comprised 23 of 50 docking runs and had an estimated binding energy of -6.16 kcal mol^{-1} (Table S1). In this orientation, the ligand is stabilized by a combination of aromatic, hydrophobic, and polar contacts distributed across the BChE active-site gorge. The heteroaromatic portion of the ligand is positioned between Trp82 and Trp430, where edge-to-face aromatic contacts are observed, while interactions with Tyr332 and Phe329 further stabilize the adjacent aromatic ring. The pyrrolidine ring is accommodated in the acyl-binding region and forms hydrophobic contacts with Phe329, Leu286, and Trp231. Importantly, in this binding mode, the carbamate moiety is not directed toward the catalytic esteratic subsite but rather toward the acyl pocket. The latter is defined mainly by Leu286, Val288, and Trp231, with the surrounding Thr284-Asn289 segment contributing to local shape complementarity. Within this region, the methyl group of the methoxy substituent is oriented toward Ser287. It approaches its side-chain region to about 3.5 Å, consistent with a stabilizing hydrophobic/van der Waals contact. Additional close contacts with residues lining the acyl pocket further support this orientation. Overall, the pose illustrates a plausible non-covalent binding mode in which the ligand is anchored primarily by

aromatic and hydrophobic interactions, whereas the carbamate group remains oriented away from the catalytic serine.

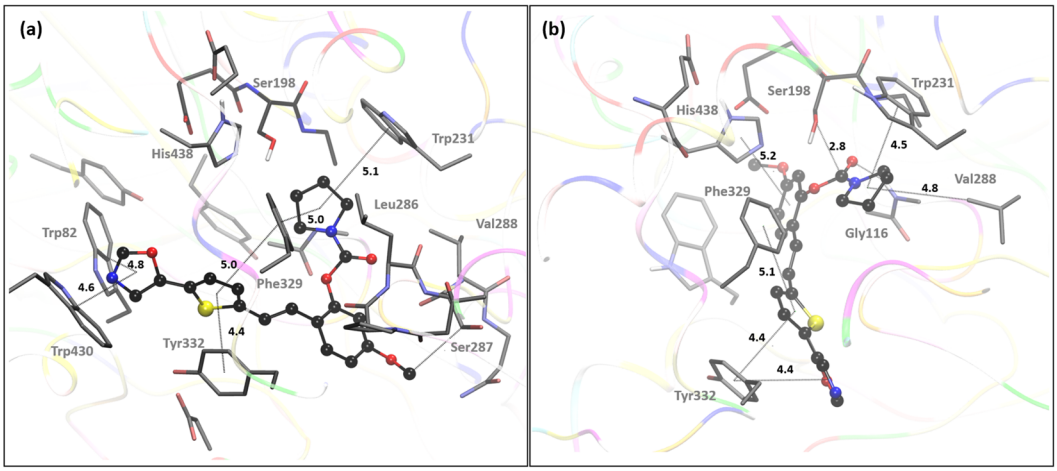


Figure 6. Representative binding modes of compound **1** in the active site of BChE (PDB ID: 1P0I) obtained by molecular docking. (**a**) Lowest-energy pose from the most populated cluster, in which the ligand is stabilized predominantly by aromatic and hydrophobic contacts within the active-site gorge. (**b**) Representative pose from the second most populated, nearly isoenergetic cluster, showing a prereactive orientation of the carbamate group toward the esteratic subdomain. Selected intermolecular distances are shown in Å.

A second, less populated but nearly isoenergetic binding mode was identified for compound **1** (Figure 6b; 9 of 50 docking runs, estimated binding energy −6.11 kcal mol^{-1}). In this orientation, the overall ligand conformation within the gorge is arranged so that the carbamate group is directed toward the esteratic subdomain, comprising the catalytic triad Ser198-His438-Glu325. The Oγ atom of Ser198 is positioned only 2.8 Å from the carbamate carbonyl carbon of the ligand, placing the non-covalent complex in a prereactive arrangement consistent with the initial step of carbamylation and subsequent covalent attachment of the ligand to the enzyme. In addition, the carbonyl oxygen is positioned toward the oxyanion-hole region, where it forms favorable contacts with the backbone NH groups of Gly116, Gly117, and Ala199. This arrangement therefore places the reactive carbamate group in a geometry compatible with formation of the covalent carbamylated enzyme. However, the docking result is interpreted here only as a plausible pre-reactive binding mode rather than as a model of the reaction pathway itself. The remainder of the ligand is stabilized by a network of aromatic and hydrophobic contacts. The central aromatic portion interacts with Tyr332 and Phe329, while the saturated pyrrolidine ring is accommodated close to Trp231 and Leu286, providing additional hydrophobic/π-alkyl stabilization. The methoxy-substituted region extends toward the Trp82 side of the gorge, contributing further van der Waals and hydrophobic contacts. Despite its lower cluster population, this pose is particularly relevant because it combines a binding energy essentially indistinguishable from that of the dominant pose with a markedly more favorable orientation of the carbamate group relative to the catalytic serine.

In the selected binding pose of compound **9**, the ligand is stabilized predominantly by a network of aromatic and hydrophobic contacts spanning the active-site gorge (Figure 7). The thiophene ring forms a favorable π-π interaction with Tyr332, with a centroid–centroid separation of approximately 4.0 Å, while the benzimidazole-bearing fragment extends toward the lower part of the gorge. The morpholine-containing carbamate region is accommodated within the acyl-pocket region, where it is supported by hydrophobic contacts with Phe329, Leu286, and Trp231. Additional stabilization is provided by the methoxy

substituent, whose methyl group is oriented toward Trp82 and forms a close alkyl-π contact. The methyl substituent on the benzimidazole ring points toward Tyr282; although this contact is weaker and more peripheral, the approximately 4.4 Å separation is consistent with a secondary hydrophobic interaction. Overall, the pose is characterized by extensive shape complementarity and dispersive/aromatic contacts rather than by a single dominant interaction, with Tyr332, Phe329, Leu286, Trp231, Trp82, and Tyr282 contributing to stabilization of the bound conformation.

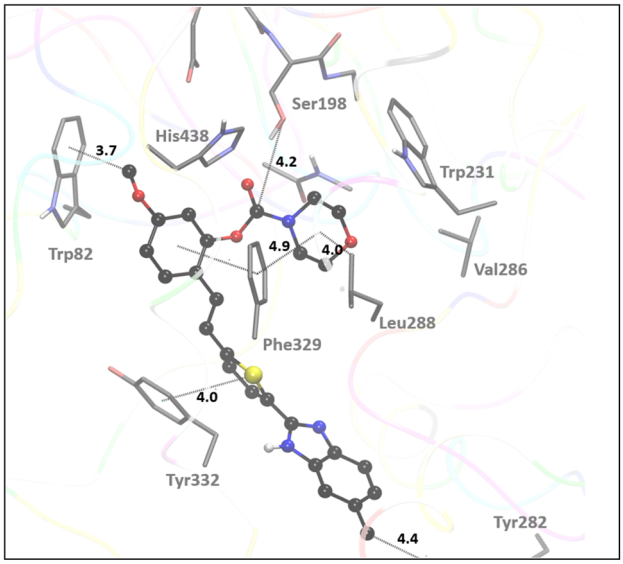


Figure 7. Representative docking pose of compound **9** in the active site of BChE. The ligand is stabilized by a network of aromatic and hydrophobic contacts involving residues lining the active-site gorge, including Tyr332, Phe329, Leu286, Trp231, Trp82, and Tyr282. Selected intermolecular distances are shown in Å.

The docking results show that both ligands can be accommodated in the BChE active site through multiple aromatic, hydrophobic, and polar contacts. Still, they exploit the available subsites in somewhat different ways. Importantly, the docking calculations are not intended to assign a unique binding mechanism or to reproduce the chemical step of inhibition, but rather to provide structurally plausible models consistent with the experimental activity. The presence of more than one energetically comparable pose for compound **1** further emphasizes the conformational adaptability of these extended carbamate inhibitors within the broad BChE active-site gorge.

4. Conclusions

A series of novel resveratrol-inspired methoxy-substituted pyrrolidine- and morpholine-based carbamates bearing oxazole or benzimidazole moieties was successfully synthesized, structurally characterized, and evaluated for their cholinesterase-inhibitory and anti-inflammatory properties. All soluble compounds of the series (**1**–**4**, **6**–**9**, and **12**) exhibited selective inhibition of BChE, while their activity toward AChE was weak or negligible. Among the derivatives investigated, pyrrolidine-based oxazole carbamate **1** showed the strongest BChE inhibitory activity, with an IC_{50} of 0.09 μM, approximately 25-fold more potent than the reference inhibitor rivastigmine. These findings further support the pyrrolidine-oxazole scaffold as a particularly favorable structural combination for selective BChE inhibition within this class of resveratrol-inspired carbamates.

Comparison with previously investigated analogs lacking the methoxy substituent showed that the effect of methoxy substitution strongly depends on the molecular scaffold. Its introduction resulted in an improvement in BChE inhibition only for compound

1, whereas a general decrease in potency was observed for most compounds in the benzimidazole series. This indicates that the methoxy group does not universally benefit BChE binding and that the ligand's overall structural arrangement governs its effect. The biological results should also be interpreted in view of the fact that compounds **1**–**12** were obtained and tested as *trans*/*cis* isomeric mixtures with or without the predominant isomer. Because the *trans*-isomers are considered more favorable for accommodation within the elongated BChE active-site gorge, varying amounts of the less active *cis*-isomer may have contributed to the observed differences in inhibitory potency. Importantly, compound **1** was the only tested derivative to inhibit TNF-α production in LPS-stimulated human PBMCs in a concentration-dependent manner, with an average IC_{50} of 4.3 μM, without affecting cell viability. The coincidence of the strongest selective BChE inhibition and measurable anti-inflammatory activity in the same compound is of particular interest in the context of the proposed relationship between the cholinergic and immune systems. However, these findings represent an initial indication of such a relationship and require further experimental investigation.

Molecular docking of representative compounds **1** and **9** further supported their ability to occupy the BChE active-site gorge through complementary aromatic, hydrophobic, and polar interactions. In particular, compound **1** exhibited more than one energetically comparable binding pose, including a conformation in which the carbamate group was favorably oriented toward the catalytic region. The docking results provide structurally plausible models consistent with the experimental inhibition data, while not establishing a unique binding mode or mechanism of inhibition.

Overall, the present results identify compound **1** as the most active member of the investigated methoxy carbamate series, combining potent and selective BChE inhibition with measurable anti-inflammatory activity and no observed effect on PBMC viability under the tested conditions. The findings also demonstrate that methoxy substitution alone is insufficient to systematically enhance biological activity, emphasizing the importance of the complete molecular architecture and stereochemical composition of these extended carbamate inhibitors. Compound **1** therefore represents a suitable lead structure for further optimization and investigation of the structural requirements underlying the combined cholinesterase-inhibitory and anti-inflammatory properties of this class of compounds.

Supplementary Materials: The following supporting information can be downloaded at https://www.mdpi.com/article/10.3390/app162110513/s1, Figures S1–S27: ^{1}H and ^{13}C NMR spectra; HRMS analysis; IC_{50} curves of BChE in the presence of carbamates **2**–**4**, **6**–**8** and **12**; Cartesian coordinates of molecules; Table S1: Free energies of binding, ΔG_{bind}, obtained by molecular docking of molecules **1**, **9**, and donepezil into the active site of BChE (PDB ID: 1P0I), together with the number of conformational clusters and conformational population distribution.

Author Contributions: Conceptualization, I.Š.; methodology, S.T., D.B. and I.Š.; investigation, M.M., T.H., A.R., T.B., S.T. and D.B.; resources, S.T., D.B. and I.Š.; writing—original draft preparation, M.M., S.T., D.B. and I.Š.; writing—review and editing, all the authors; supervision, I.Š. All authors have read and agreed to the published version of the manuscript.

Funding: The research was supported by the Federal Ministry of Education and Science of Bosnia and Herzegovina, grant No. 05-35-3512-1/25.

Institutional Review Board Statement: Not applicable.

Informed Consent Statement: Not applicable.

Data Availability Statement: The data are available from the authors on request.

Acknowledgments: We thank the University of Zagreb (Croatia) Computing Center (SRCE) for granting computational time on the Supercomputer Supek. The authors thank Željka Rupčić from

Selvita Ltd. for kindly performing the HRMS analyses. We also acknowledge Sunčica Roca from the NMR Center at Ruđer Bošković Institute for recording all the NMR spectra and Martina Bosnar for supervising the anti-inflammatory activity tests. We also acknowledge support from Pharmacology in vitro, Selvita Ltd.

Conflicts of Interest: Tea Bruketa was employed by the Selvita Ltd. The rest of the authors declare no conflict of interest.

References

1. Martelli, D.; McKinley, M.J.; McAllen, R.M. The cholinergic anti-inflammatory pathway: A critical review. *Auton. Neurosci.* **2014**, *182*, 65–69. [CrossRef] [PubMed]
2. Pavlov, V.A.; Wang, H.; Czura, C.J.; Friedman, S.G.; Tracey, K.J. The cholinergic anti-inflammatory pathway: A missing link in neuroimmunomodulation. *Mol. Med.* **2003**, *9*, 125–134. [CrossRef] [PubMed]
3. Hu, S.; Wang, Y.; Li, H. The regulation effect of a7nAChRs and M1AChRs on inflammation and immunity in sepsis. *Mediat. Inflamm.* **2021**, *2021*, 9059601. [CrossRef] [PubMed]
4. Pohanka, M. Inhibitors of acetylcholinesterase and butyrylcholinesterase meet immunity. *Int. J. Mol. Sci.* **2014**, *15*, 9809–9825. [CrossRef] [PubMed]
5. Pohanka, M. Alpha7 nicotinic acetylcholine receptor is a target in pharmacology and toxicology. *Int. J. Mol. Sci.* **2012**, *13*, 2219–2238. [CrossRef] [PubMed]
6. Rosas-Ballina, M.; Tracey, K.J. Cholinergic control of inflammation. *J. Intern. Med.* **2009**, *265*, 663–679. [CrossRef] [PubMed]
7. Bernik, T.R.; Friedman, S.G.; Ochani, M.; DiRaimo, R.; Ulloa, L.; Yang, H.; Sudan, S.; Czura, C.J.; Ivanova, S.M.; Tracey, K.J. Pharmacological stimulation of the cholinergic anti-inflammatory pathway. *J. Exp. Med.* **2002**, *195*, 781–788. [CrossRef] [PubMed]
8. Borovikova, L.V.; Ivanova, S.; Zhang, M.H.; Yang, H.; Botchkina, G.I.; Watkins, L.R.; Wang, H.C.; Abumrad, N.; Eaton, J.W.; Tracey, K.J. Vagus nerve stimulation attenuates the systemic inflammatory response to endotoxin. *Nature* **2000**, *405*, 458–462. [CrossRef] [PubMed]
9. Andersson, U.; Tracey, K.J. Neural reflexes in inflammation and immunity. *J. Exp. Med.* **2012**, *209*, 1057–1068. [CrossRef] [PubMed]
10. Pavlov, V.A.; Ochani, M.; Gallowitsch-Puerta, M.; Ochani, K.; Huston, J.M.; Czura, C.J.; Al-Abed, Y.; Tracey, K.J. Central muscarinic cholinergic regulation of the systemic inflammatory response during endotoxemia. *Proc. Natl. Acad. Sci. USA* **2006**, *103*, 5219–5223. [CrossRef] [PubMed]
11. Pavlov, V.A.; Parrish, W.R.; Rosas-Ballina, M.; Ochani, M.; Puerta, M.; Ochani, K.; Chavan, S.; Al-Abed, Y.; Tracey, K.J. Brain acetylcholinesterase activity controls systemic cytokine levels through the cholinergic anti-inflammatory pathway. *Brain Behav. Immun.* **2009**, *23*, 41–45. [CrossRef] [PubMed]
12. Wang, H.; Yu, M.; Ochani, M.; Amella, C.A.; Tanovic, M.; Susarla, S.; Li, J.H.; Wang, H.C.; Yang, H.; Ulloa, L.; et al. Nicotinic acetylcholine receptor alpha 7 subunit is an essential regulator of inflammation. *Nature* **2003**, *421*, 384–388. [CrossRef] [PubMed]
13. Jarczyk, J.; Yard, B.A.; Hoeger, S. The cholinergic anti-inflammatory pathway as a conceptual framework to treat inflammation-mediated renal injury. *Kidney Blood Press. Res.* **2019**, *44*, 435–448. [CrossRef] [PubMed]
14. Milena, M.; Milić, S.; Talić, S.; Šagud, I.; Bruketa, T.; Bosnar, M.; Barić, D.; Odak, I.; Škorić, I. Design, computational study, and biological assessment of novel benzimidazole and oxazole derivatives of morpholine and pyrrolidine carbamates incorporating a diarylethene motif. *Bioorg. Chem.* 2026; in the process of publication. [CrossRef]
15. Mlakić, M.; Odak, I.; Faraho, I.; Talić, S.; Bosnar, M.; Lasić, K.; Barić, D.; Škorić, I. New naphtho/thienobenzo-triazoles with interconnected anti-inflammatory and cholinesterase inhibitory activity. *Eur. J. Med. Chem.* **2022**, *241*, 114616. [CrossRef] [PubMed]
16. Ellman, G.L.; Courtney, K.D.; Andres, V.; Featherstone, R.M. A new and rapid colorimetric determination of acetylcholinesterase activity. *Biochem. Pharmacol.* **1961**, *7*, 88–95. [CrossRef] [PubMed]
17. Frisch, M.J.; Trucks, G.W.; Schlegel, H.B.; Scuseria, G.E.; Robb, M.A.; Cheeseman, J.R.; Scalmani, G.; Barone, V.; Petersson, G.A.; Nakatsuji, H.; et al. *Gaussian 16*; Revision C.01; Gaussian, Inc.: Wallingford, CT, USA, 2016.
18. Morris, G.M.; Huey, R.; Lindstrom, W.; Sanner, M.F.; Belew, R.K.; Goodsell, D.S.; Olson, A.J. AutoDock4 and AutoDockTools4: Automated docking with selective receptor flexibility. *J. Comput. Chem.* **2009**, *16*, 2785–2791. [CrossRef] [PubMed]
19. Nicolet, Y.; Lockridge, O.; Masson, P.; Fontecilla-Camps, J.C.; Nachon, F. Crystal structure of human butyrylcholinesterase. *PDB* **2003**. [CrossRef]
20. Terali, K.; Dalmizrak, O.; Uzairu, S.M.; Ozer, N. New insights into the interaction between mammalian butyrylcholinesterase and amitriptyline: A combined experimental and computational approach. *Turk. J. Biochem.* **2019**, *44*, 55–61. [CrossRef]
21. Mlakić, M.; Odak, I.; Barić, D.; Talić, S.; Šagud, I.; Štefanić, Z.; Molčanov, K.; Lasić, Z.; Kovačević, B.; Škorić, I. New resveratrol analogs as improved biologically active structures: Design, synthesis and computational modeling. *Bioorg. Chem.* **2024**, *143*, 106965. [CrossRef] [PubMed]
22. Kikaš, I.; Škorić, I.; Marinić, Ž.; Šindler-Kulyk, M. Synthesis and phototransformations of novel styryl-substituted furobenzobicyclo[3.2.1]octadiene derivatives. *Tetrahedron* **2010**, *66*, 9405–9414. [CrossRef]

23. Horspool, W.M.; Song, P.S. *CRC Handbook of Organic Photochemistry and Photobiology*; CRC Press: Boca Raton, FL, USA, 1995.
24. Griesbeck, A.; Oelgemöller, M.; Ghetti, F. *CRC Handbook of Organic Photochemistry and Photobiology*, 3rd ed.; CRC Press: Boca Raton, FL, USA, 2012.

Disclaimer/Publisher's Note: The statements, opinions and data contained in all publications are solely those of the individual author(s) and contributor(s) and not of MDPI and/or the editor(s). MDPI and/or the editor(s) disclaim responsibility for any injury to people or property resulting from any ideas, methods, instructions or products referred to in the content.